Available online at www.sciencedirect.com
SCIENCE DIRECT®
Journal of Magnetic Resonance 165 (2003) 102–115
JMR Journal of Magnetic Resonance
www.elsevier.com/locate/jmr

PFG-assisted selection and suppression of ^{1}H NMR signals in the solid state under fast MAS

Ingrid Fischbach, Karena Thieme, Anke Hoffmann, Manfred Hehn, and Ingo Schnell*

Max-Planck Institut für Polymerforschung, Postfach 3148, D-55021 Mainz, Germany

Received 7 May 2003; revised 18 July 2003

Communicated by Lucio Frydman

Abstract

Under fast MAS conditions, techniques for ^{1}H signal selection and suppression, which have originally been developed for solution-state NMR, become applicable to solids. In this work, we describe how WATERGATE and DANTE pulse sequences can be used under MAS to selectively excite or suppress peaks in ^{1}H solid-state spectra. As known from the liquid-state analogues, signal selection and/or suppression is supported by pulsed-field gradients which selectively dephase and rephase transverse magnetisation. Under MAS, the required field gradients are provided by a simple pair of coils which have been built into a standard fast-MAS probe. PFG-assisted techniques enable efficient selection or suppression of ^{1}H peaks in a single transient of the pulse sequence without the need for phase cycles. Therefore, these tools can readily be incorporated into solid-state MAS NMR experiments, which is demonstrated here for ^{1}H–^{1}H double-quantum NMR spectra of supramolecular systems. In the examples presented here, the ^{1}H signals of interest are relatively weak and need to be observed despite the presence of the strong ^{1}H signal of long alkyl sidechains. PFG-assisted suppression of this strong perturbing signal is shown to be particularly useful for obtaining unambiguous results.

Keywords: Solid-state ^{1}H NMR; Pulsed field-gradients; Fast MAS; Peak suppression; Peak selection

1. Introduction: DANTE and WATERGATE techniques

In modern high-resolution NMR, techniques for selective excitation [1–4] and/or suppression [5,6] of peaks belong to the standard tools and are routinely available on spectrometers. Many variants of such techniques have been developed on the basis of frequency-selective pulses in Fourier transform NMR [7,8]. In principle, the excitation bandwidth of such pulses is deliberately reduced by extending the time of application, because the pulses' excitation spectrum is reflected by the Fourier transform of the pulse envelope. Thus, in the simplest form, frequency-selective pulses are long rectangular or Gaussian-shaped pulses [7] with the transmitter being set to the resonance frequency of interest. To efficiently select the wanted signals and, at the same time, remove the unwanted ones from the spectrum, pulsed field-gradients (PFGs) have been introduced to the experiments, [9–11] which dephase coherences of unwanted spin signals, while the signals of the wanted coherences are constructively refocused.

Frequency-selective excitation can also be accomplished by combining "hard" non-selective pulses with nutation delays, during which the spins effectively precess with a frequency $\Delta\omega^{(i)} = \omega^{(i)} - \omega_0$, where $\omega^{(i)}$ and ω_0, are the resonance frequency of the spin i and the carrier frequency of the pulses, respectively. In the simplest case, two $\pi/2$ pulses separated by a delay of $\tau = 2/(\pi\Delta\omega^{(i)})$ can be used to select or suppress the signal of the spins i [12,13]. In a more elaborate form, the same principle forms the basis for DANTE-type selective pulses introduced by Bodenhausen, Freeman and Morris [14,15]. Due to its simplicity and robustness, we have used DANTE-type π-pulses for frequency-selective inversion of spins in the solid state (see below). In essence, the selective inversion pulse is part of a spin–echo sequence of the form $(\pi/2) - \tau - (\pi)_{\mathrm{DANTE}} - \tau -$ acqu.

* Corresponding author. Fax: +49-6131-379-320.
E-mail address: schnelli@mpip-mainz.mpg.de (I. Schnell).

1090-7807/$ - see front matter © 2003 Elsevier Inc. All rights reserved.
doi:10.1016/j.jmr.2003.07.002

where two identical PFGs are applied during the two echo delays τ. In this way, the PFGs refocus only the signal of the spins that are inverted by the selective π-pulse, while the signal of all other spins is removed from the spectrum.

A particularly successful variant of this experimental scheme is represented by the WATERGATE technique introduced by Piotto, Saudek and Sklenar [16,17]. The frequency-selective inversion pulse consists of a sequence of six pulses with durations of $3\alpha - 9\alpha - 19\alpha - 19\alpha - 9\alpha - 3\alpha$ with $26\alpha = \pi$, which follows the concept of binomial pulses [18,19] and is usually referred to as a "3–9–19 pulse" [17,20]. Effectively, this binomial sequence inverts all resonances within the spectrum except for the frequencies $\omega^{(k)} = 2\pi k/\tau_\alpha$, where k is an integer (including zero) and τ_α is the delay between two pulses of the binomial sequence. In combination with two identical PFGs applied before and after the 3–9–19 pulse, WATERGATE efficiently suppresses the signal located at the carrier frequency of the pulse train as well as all signals at $\omega^{(k)} = 2\pi k\tau_\alpha$, because all these signals are dephased twice by the PFGs, while all other signals are refocused. In principle, any selective π-pulse, together with an appropriate combination of two PFGs, would serve the same purpose, but experimentally the 3–9–19 pulse has proven to be particularly robust and tolerant with respect to slight misadjustments.

Apart from the approaches mentioned above, numerous frequency-selective pulse schemes have been developed, which employ, for example, shaped pulses [21] or amplitude- and frequency-modulated pulses that are optimised via numerical simulations [22,23]. In comparison to DANTE-type sequences, they are usually more demanding and rely more strongly on experimental conditions typically encountered in liquid-/solution-state NMR. Therefore, they cannot be adapted to solid-state NMR and fast-MAS conditions as straightforwardly as the DANTE and WATERGATE techniques, which merely consist of a small number of hard pulses plus PFGs for signal dephasing and rephasing.

2. Technical requirements: pulsed-field gradients in fast-MAS probes

While the DANTE and WATERGATE pulses provide frequency-selective inversion of signals, PFGs are required to efficiently suppress NMR signals by dephasing and rephasing. In high-resolution NMR, PFGs are well-established tools for selection of coherence transfer pathways in general [9,10]. Their particular advantage over pulse phase cycling schemes is that they develop their effect within a single transient of the pulse sequence. Consequently, signal averaging over a number of consecutive transients—as commonly performed in the course of pulse phase cycling schemes—can be avoided, which helps to reduce experiment time requirements and, moreover, allows the dynamic range of the signal receiving unit to be optimally adjusted to the incoming signal of interest.

In solid-state NMR, however, PFGs are relatively rarely used [24–27] because their usual application times are in the order of 1 ms and, thus, relatively long as compared to transverse relaxation times of solids. Transverse spin states, which are required for PFGs to take effect, tend to be subject to strong spin–spin relaxation so that the signal largely disappears before a dephasing/rephasing cycle is completed. Hence, PFGs need to be combined with decoupling techniques that efficiently average the interactions responsible for the relaxation mechanisms, i.e. predominantly dipole-dipole couplings in spin–1/2 systems. In heteronuclear ^{1}H–X systems, conventional ^{1}H decoupling pulses would serve this purpose, but due to the action of the field gradient the decoupling bandwidth has to be correspondingly broad, which is usually beyond the capabilities of available decoupling pulse schemes. In addition, radio-frequency pulses and field gradient pulses would have to be applied at the same time, which also makes high demands on the NMR probe electronics; in particular, coupling phenomena between the individual circuits need to be prevented.

Magic-angle spinning (MAS), in contrast, does not give rise to such interference problems with PFGs, and therefore appears as the method of choice to overcome transverse relaxation problems and, in particular, provide spectral resolution. Since MAS also averages effects arising from sample inhomogeneity, such as susceptibility gradients, it has recently been introduced into high-resolution NMR spectroscopy of partially mobile and heterogeneous systems. The combination of standard high-resolution NMR experiments with MAS is often referred to as "high-resolution MAS" (HRMAS) [28–30] and has attracted considerable interest [31–33] e.g., for the on-bead characterisation of peptides in solid-phase synthesis or for investigations of tissue samples in medical applications. Of course, for such high-resolution NMR experiments PFGs are an indispensable tool, so that in the meantime HRMAS probes have become commercially available with a pair of PFG coils wrapped around the MAS stator. Typically, rotors of around 4 mm outer diameter are used for HRMAS experiments, because usually the partially mobile character of the materials requires only moderate MAS frequencies ($<$10 kHz).

In order to make PFGs and PFG-based experiments available for solid-state NMR spectroscopy, it appears obvious to follow the HRMAS approach and to extend it to higher MAS frequencies. Therefore, we have built a pair of PFG coils into a Bruker fast-MAS probe (of standard-bore size) supporting rotors of 2.5 mm outer diameter. The principal design of PFG coils in MAS probes is known from the work of Maas et al. [34].

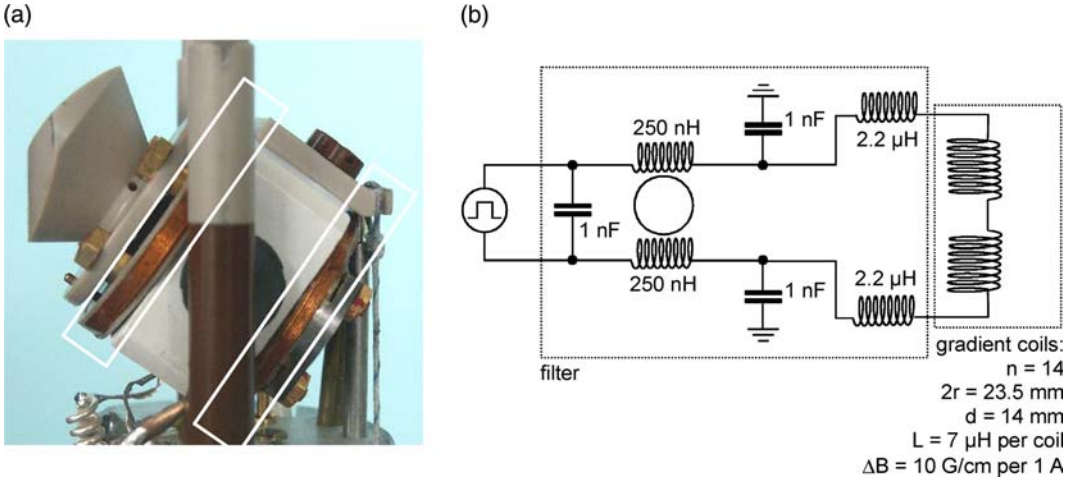

Fig. 1. (a) Pair of field-gradient coils attached to the top and the bottom of a Bruker 2.5 mm fast-MAS stator in a commercial ^{1}H–X double-resonance probehead with a standard bore diameter (54 mm). (b) Circuit including the pair of field-gradient coils (arranged in an anti-Helmholtz fashion) and a frequency filter that avoids coupling of the gradient circuit with the RF circuits of the probe. The details of the gradient coils are given in the inset (n, number of windings; $2r$, coil diameter; d, separation of the two coils; L, inductance).

Ideally, the gradient should be oriented such that (i) the z component of the magnetic field increases along the spinning axis and (ii) the z component of the field gradient is uniform in the planes perpendicular to the spinning axis. To meet these criteria, however, a special coil geometry is required, which includes modifications to the MAS stator. To reduce the technical efforts to a minimum and to keep the MAS stator unaltered, a less elaborate design is used in the work presented here. Two ring-shaped coils (consisting of 14 windings each) are attached to the top and the bottom of the MAS stator with the rotor axis perpendicular to the coils (see photograph and circuit diagram in Fig. 1). The windings are arranged in an anti-Helmholtz fashion, resulting in a field gradient over the sample volume. Due to the simple coil design, the resulting field gradient is not perfectly oriented along the rotor axis. However, since the coils are used for basic dephasing and rephasing purposes, they only need to provide a reproducible field gradient which is sufficiently strong to dephase NMR signals on the timescale of fast MAS experiments.

From a practical point of view, it is relatively simple to attach the gradient coils to the top and the bottom of the MAS stator, but this arrangement comes at the price of considerable coupling between the two gradient coils and the RF coil in the center of the stator, as all three coils induce parallel magnetic fields. Without further precautions taken, this would in particular lead to significant energy losses of the high-power pulses applied on the RF circuit, because the pulsed RF fields would be taken up to a considerable extent by the gradient coils. Therefore, frequency filters need to be built into the gradients' circuit, which prevent the reception and dissipation of pulsed RF fields. The full gradients' circuit diagram is shown in Fig. 1b. In the filter part, the two strongly coupled coils together with the three capacitors effectively constitute a standard low-pass filter which removes all frequencies >1 MHz and thus allows sine-shaped gradient pulses as short as 1 μs to pass. The two other non-coupled coils act as an additional support for suppressing high frequencies. As a whole, the filter ensures an attenuation of >40 dB between the gradient circuit and the RF circuits.

Under MAS conditions, the gradient pulses need to be applied on the time scale of rotor periods, $t_R = 1/\nu_R$. For solid-state ^{1}H NMR, MAS frequencies of $\nu_R > 25$ kHz are desirable, and in the experiments presented in this work ν_R was set to 30 kHz. Therefore, gradient pulses of durations $p_G = 1, \ldots, 10t_R$, corresponding to $p_G = 33, \ldots, 333$ μs, need to be available at sufficient strengths. With the gradient circuit detailed above, sine-shaped gradient pulses with $p_G \geqslant 100$ μs and field gradients of $\Delta B \leqslant 50$ G/cm could be achieved, applying currents of up to 5 A. Before recording the NMR signal after such gradient pulses, a ring-down delay of ~100 μs is required. As the coil geometry used in this work is not perfectly adapted to MAS conditions (see above), the gradient strength and, thus, the dephasing effect as experienced by a volume fraction of the sample might slightly vary in the course of the rotation. To partially compensate for this imperfection, the gradient pulses should be applied for at least two rotor periods duration, i.e. $p_G \geqslant 2\ t_R = 66$ μs at 30 kHz MAS.

3. Experimental schemes for solid-state MAS NMR

In the following, three PFG-assisted pulse sequences will be described in detail (see Fig. 2), which provide selective suppression or excitation of ^{1}H signals in

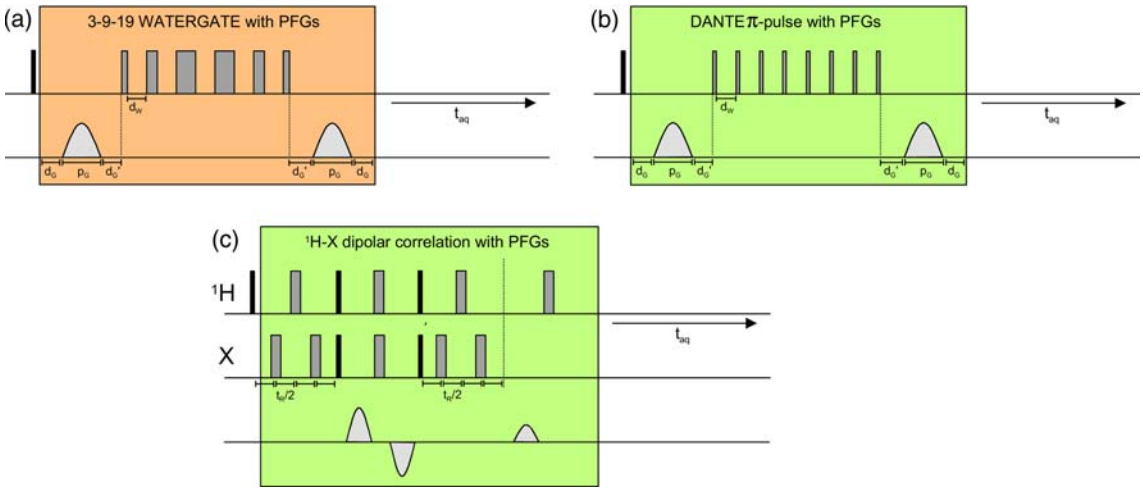

Fig. 2. PFG-assisted pulse sequences applied for selective excitation or suppression of ^{1}H resonances in ^{1}H NMR spectra under fast MAS. (a) WATERGATE sequence for selective peak suppression, using a 3–9–19 inversion pulse and a pair of pulsed field gradients. (b) Sequence for selective excitation using a DANTE inversion pulse and a pair of pulsed field gradients that only refocus the inverted resonance. At 30 kHz MAS, typical timings and settings for the WATERGATE and DANTE sequences are $d_G = 33$ μs, $p_G = 100$ μs, $d'_G = 100$ μs, $d_W = 33$ or 67 μs, $\Delta B = 20, \ldots, 30$ G/cm. (c) Heteronuclear ^{1}H–X dipolar filter sequence consisting of two REDOR-type dipolar recoupling blocks that are separated by a period of transverse X-spin magnetisation. During this period, PFGs dephase ^{1}H–X correlations which are, before detection, rephased on the ^{1}H side. In this way, the signal of protons attached to a X nucleus (^{13}C or ^{15}N) is selected. The experiment is based on ^{1}H–X dipole–dipole couplings, but works analogously to gradient-selected HSQC-type experiments known from high-resolution NMR.

solid-state MAS spectra. The two homonuclear sequences are based on the concepts of WATERGATE [16,17] and DANTE, while the heteronuclear variant employs a dipolar ^{1}H–X filter based on REDOR-type recoupling [35–37] for selection of protons directly attached to isotopically labelled heteronuclei, such as ^{13}C or ^{15}N.

The performance of the pulse sequences is demonstrated on a sample of imidazolium-methylsulfonate, the chemical structure of which is depicted in Fig. 3. Under MAS at 30 kHz, this material shows four clearly resolved ^{1}H resonance lines (the assignment is given in Fig. 4a). The nitrogen positions are fully ^{15}N-enriched in order to demonstrate the selection performance of the heteronuclear ^{1}H–^{15}N filter. The experiments were performed on a Bruker Avance spectrometer operating at Larmor frequencies of 700.1 and 70.9 MHz for ^{1}H and ^{15}N, respectively. All RF pulses were applied at a transverse B_1 field of 100 kHz, corresponding to a $\pi/2$-pulse width of 2.5 μs. During ^{1}H acquisition, no additional ^{15}N RF decoupling was required due to the decoupling performance of 30 kHz MAS.

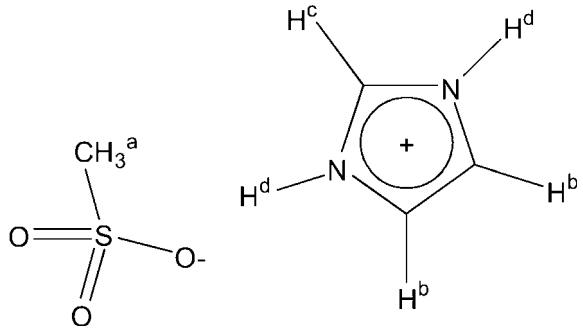

Fig. 3. Chemical structure of imidazolium-methylsulfonate with the four distinguishable types of protons being indicated by superscripts a–d.

3.1. WATERGATE-type peak suppression

To accomplish selective peak suppression, the WATERGATE sequence with a 3–9–19 pulse is adapted to fast MAS conditions. According to the chosen RF power level, the segments of the 3–9–19 pulse are 0.58, 1.73 and 3.65 μs long. The separation of the pulses (d_W in Fig. 2a) determines the frequency bandwidth of the suppression. Experimentally, an approximate synchronisation of these delays with the rotor period has turned out to be advantageous, but not necessary. Depending on the linewidth of the peak to be suppressed, d_W is typically varied between $t_R/2$ and $2t_R$, which corresponds to $16.7, \ldots, 66.7$ μs, when a MAS frequency of 30 kHz is used.

In Fig. 4a, the suppression efficiency of the MAS-adapted WATERGATE sequence is shown for the ^{1}H spectrum of imidazolium-methylsulfonate. Each of the four peaks (with the assignment given on top of Fig. 4a) can individually be suppressed without significantly distorting the rest of the spectrum. Best selectivity was achieved with a pulse spacing of $d_W = 2t_R = 66.7$ μs. Gradient pulses of $p_G = 200$ μs were applied, bracketed by delays of $d_G = 100$ μs and $d'_G = 33.3$ μs. Using currents of $2, \ldots, 3$A, signal dephasing occurred in the presence of field gradients of $\Delta B = 20, \ldots, 30$ G/cm.

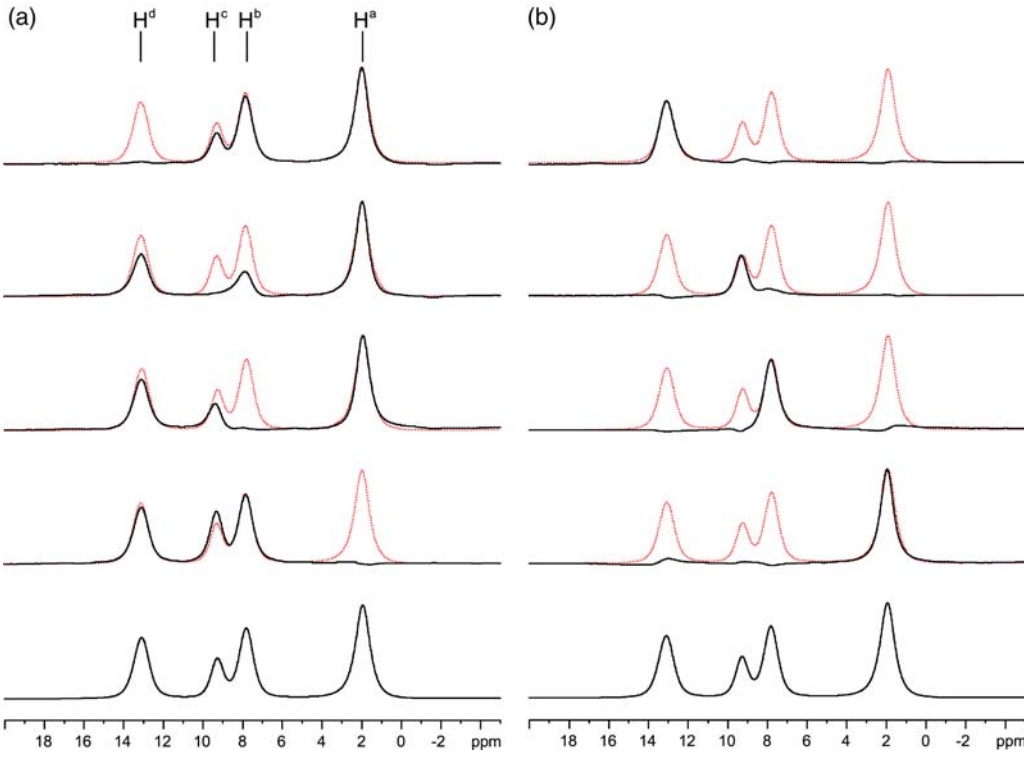

Fig. 4. Single-transient ^{1}H MAS spectra of imidazolium-methylsulfonate. (a) Selective suppression of ^{1}H resonances by the PFG-assisted WATERGATE sequence depicted in Fig. 2a. From the top to the bottom, each of the four peaks is selectively suppressed. (b) Selective excitation of ^{1}H resonances by the PFG-assisted DANTE spin–echo sequence depicted in Fig. 2b. From the top to the bottom, each of the four peaks is selectively excited. For comparison, the full ^{1}H spectrum is given at the bottom and as a red dotted line behind all other spectra.

Most importantly, it is to be noted that each spectrum shown in Fig. 4 is the result of a *single* transient of the pulse sequence. The PFGs ensure practically complete dephasing of the selected signals and remove the unwanted peaks, leaving a noise level on the order of 1% of the original signal intensity. No further phase cycling is needed to obtain clean spectra, which allows the sequence to be readily incorporated into other experiments without the need for extending their phase cycle.

3.2. Selective excitation using a DANTE pulse

After presenting a PFG-assisted technique for peak suppression, we now turn to its counterpart, i.e. a sequence for selective excitation of individual peaks. For this purpose, a gradient spin–echo sequence with a selective DANTE π-pulse was adapted to 30 kHz MAS conditions. Best results were obtained for a DANTE pulse consisting of eight segments (each of 0.63 μs duration) separated by delays of $d_W = t_R = 33.3$ μs. The gradient pulses were applied identically to the WATERGATE sequence described above, i.e., $p_G = 200$ μs, $d_G = 100$ μs, $d'_G = 33.3$ μs and $\Delta B = 20$ G/cm.

In Fig. 4b, resulting ^{1}H spectra of imidazolium-methylsulfonate are shown, in which each of the four peaks is separately excited. Again, the spectra result from single transients of the PFG-assisted DANTE sequence. The intensity of the unwanted peaks is effectively reduced to less than 5% of the original peak intensity. This suppression efficiency is sufficient for most applications, but a bit less than what was obtained by the WATERGATE technique discussed above. This shows that the simple DANTE approach employed here still has potential for further optimisation and enhancement, for example by implementing more sophisticated inversion pulse schemes [38].

3.3. Selective excitation using a heteronuclear dipolar ^1H–X filter

The homonuclear schemes for peak-selective excitation and suppression discussed so far are based on frequency-selective pulses and their narrow-band signal inversion. An alternative means of selection are heteronuclear ^{1}H–X correlations which pick out protons that are directly attached to the chosen NMR-active heteronucleus. In principle, this gradient selection procedure is identical to the one established for heteronuclear single-quantum correlation (HSQC) experiments in high-resolution NMR [10]. It starts with the formation of heteronuclear ^{1}H–X correlations, which are then dephased by applying PFGs on a transverse state of the X spins (while the ^{1}H spins adopt longitudinal states in the ^{1}H–X correlation and are thus insensitive to the

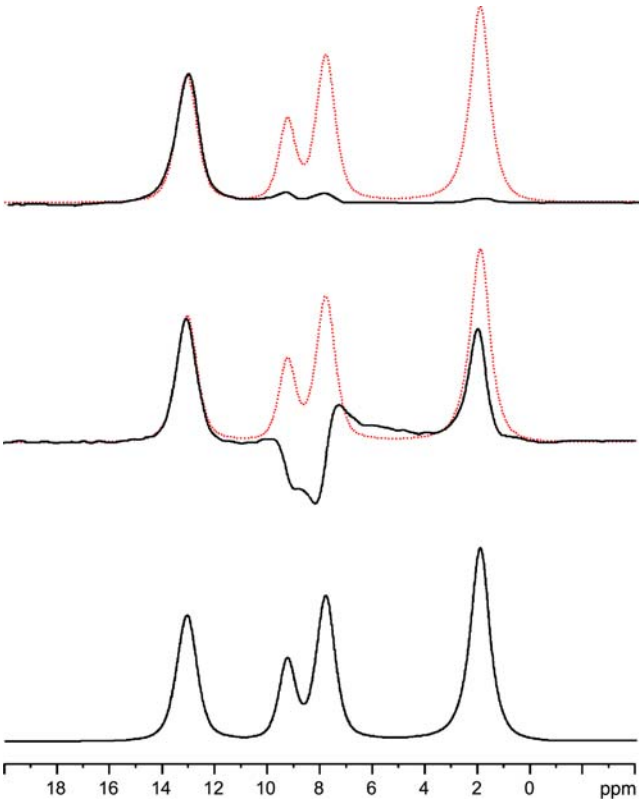

Fig. 5. ^{1}H peak selection in ^{15}N-enriched imidazolium-methylsulfonate by the heteronuclear dipolar ^{1}H–^{15}N filter sequence depicted in Fig. 2c. Full filter efficiency is achieved when PFGs are combined with a two-step pulse phase cycle that alternates the phase of one of the $\pi/2$ pulses applied to ^{15}N (top spectrum). The two-step phase cycle without the PFGs, however, would not provide sufficient selection (middle spectrum). The full ^{1}H spectrum is given at the bottom and, for comparison, as a red dotted line behind the spectra.

PFGs). After reconverting the ^{1}H–X correlations to ^{1}H magnetisation, the signals are rephased by a PFG (now acting on ^{1}H transverse magnetisation) before detection. The PFG durations and amplitudes need to be chosen such that the integral over all gradient pulses applied on X-spin transverse states is by a factor of γ_{1H}/γ_{X} larger than the integral of the gradient pulse applied on the detected ^{1}H transverse magnetisation.

In high-resolution NMR of mobile solubilised molecules J-couplings are commonly used to generate such "through-bond" ^{1}H–^{13}C or ^{1}H–^{15}N correlations, whereas in solids dipole–dipole couplings exceed the J-couplings by roughly two orders of magnitude and, thus, appear to be the first choice. Under MAS, dipolar ^{1}H–X correlations are conveniently produced by recoupling the dipole–dipole coupling in a REDOR-type fashion [35–37]. A variety of experiments including REDOR- or TEDOR-type [39] dipolar recoupling have been proposed, including dipolar ^{1}H–^{13}C or ^{1}H–^{15}N HSQC spectra [40–42], which are largely analogous to their solution-state counterparts. Even the concepts of sensitivity enhancement by inverse, i.e., ^{1}H, detection schemes have already been adapted from high-resolution conditions to solid-state NMR under fast MAS [43–45]. In these solid-state experiments, the wanted signals and coherence transfer pathways have been selected by means of RF pulse-phase cycles and dephasing pulses [44]. Recently, ^{1}H–^{15}N CP-TEDOR and other dipolar ^{1}H–^{15}N correlation experiments have been introduced [46,47], which realise inverse (^{1}H) detection in the solid state under fast MAS with the aid of the PFGs described in this work.

In this context, the PFG-assisted dipolar ^{1}H–X filter is mentioned here as an alternative means of ^{1}H peak selection. The results obtained on ^{15}N-enriched imidazolium-methylsulfonate are shown in Fig. 5. In contrast to the homonuclear WATERGATE and DANTE procedures, a single transient of the sequence does not yet yield a satisfactory suppression of the unwanted ^{1}H peaks. The selection performance of the PFGs alone is obviously not sufficient and needs to be supplemented by a two-step phase cycle in which the phase of one of the two $\pi/2$ pulses on ^{15}N is alternated together with the receiver. This phase alternation provides cancellation of ^{1}H signal contributions that did not pass through a ^{1}H–^{15}N correlation. However, without the help of the PFGs, the two-step phase cycle alone would not yield clean spectra either (see Fig. 5, middle spectrum). Only the combination of PFGs with a two-step RF pulse-phase alternation provides sufficient suppression of the unwanted ^{1}H signals, leaving residual signals of $<3\%$ of the original signal intensities (see Fig. 5, top spectrum).

4. Incorporation into 2D ^{1}H–^{1}H double-quantum NMR

Having demonstrated the selection or suppression efficiency of PFG-assisted WATERGATE and DANTE sequences, we now turn to examples that show how simply and efficiently these techniques can be incorporated into existing solid-state ^{1}H NMR experiments. For this purpose, two-dimensional ^{1}H–^{1}H double-quantum (DQ) NMR spectra have been chosen, but any other ^{1}H–^{1}H (or ^{1}H–X) correlation experiment performed under fast MAS would be equally well suited.

^{1}H–^{1}H DQ NMR spectroscopy is based on the generation of ^{1}H–^{1}H DQ coherences via homonuclear dipole–dipole couplings [48]. Consequently, the intensity of a DQ signal sensitively depends on the coupling between the respective pair of nuclei. Therefore, DQ signals are indicative of internuclear distances as well as molecular motions. Under MAS conditions, dipolar recoupling pulse sequences are applied to excite DQ coherences and, subsequently, to reconvert them back into observable magnetisation. In this work, we have used the simple back-to-back sequence [48,49] (depicted in Fig. 6a) which proved to be extremely robust under

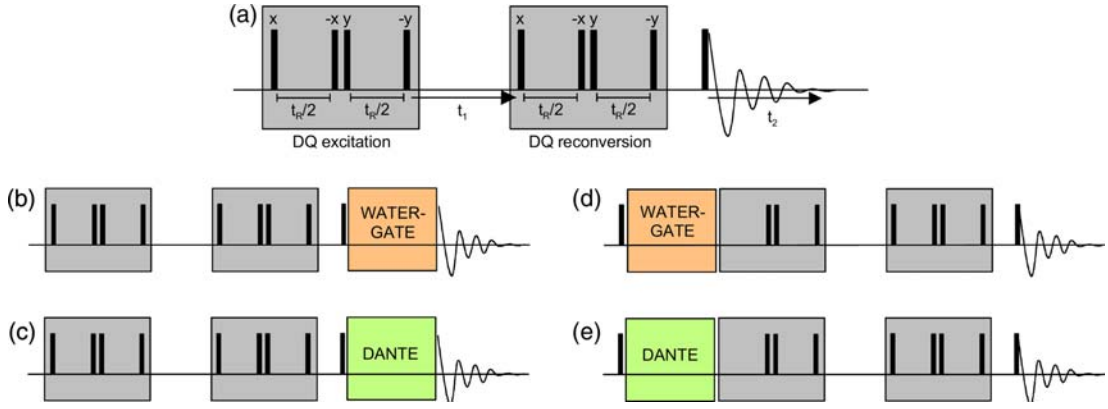

Fig. 6. (a) Back-to-back pulse sequence for ^{1}H–^{1}H double-quantum MAS NMR spectroscopy. Homonuclear dipolar recoupling is applied for exciting double-quantum coherences involving two dipolar-coupled protons, and subsequently for reconverting the coherence back to observable magnetisation. In this way, a ^{1}H–^{1}H double-quantum dimension (t_1) is correlated with a usual ^{1}H single quantum dimension (t_2). (b)–(d) Modified pulse sequences for ^{1}H–^{1}H double-quantum spectroscopy with (b) selective suppression or (c) selective detection of signals in t_2, or with (d) selective suppression or (e) selective excitation of double-quantum coherences.

fast MAS. Two nested phase cycles consisting of four steps each are used to select the coherence transfer pathway $0 \rightarrow \pm 2 \rightarrow 0 \rightarrow -1$ with an overall 16-step phase cycle. With the experimental conditions applied (MAS at 30 kHz, DQ excitation and reconversion for one rotor period), ^{1}H–^{1}H DQ signals are expected in a solid material for all proton pairs with a distance of less than ~0.35 nm. In the resulting two-dimensional DQ spectra, a DQ dimension is correlated with a conventional single-quantum (SQ) dimension. In the DQ dimension, the chemical shift of the signals corresponds to the sum of the chemical shifts of the two nuclei involved in the DQ coherence: $\omega_{AB} = \omega_A + \omega_B$. In the SQ dimension, the signal splits up into the two single-spin resonances, ω_A and ω_B, so that for $\omega_A \neq \omega_B$ pairs of signals located at $(\omega_A + \omega_B, \omega_A)$ and $(\omega_A + \omega_B, \omega_B)$ are observed in the DQ spectrum, while for $\omega_A = \omega_B$ a single peak is found at $(2\omega_A, \omega_A)$ on the so-called DQ "diagonal".

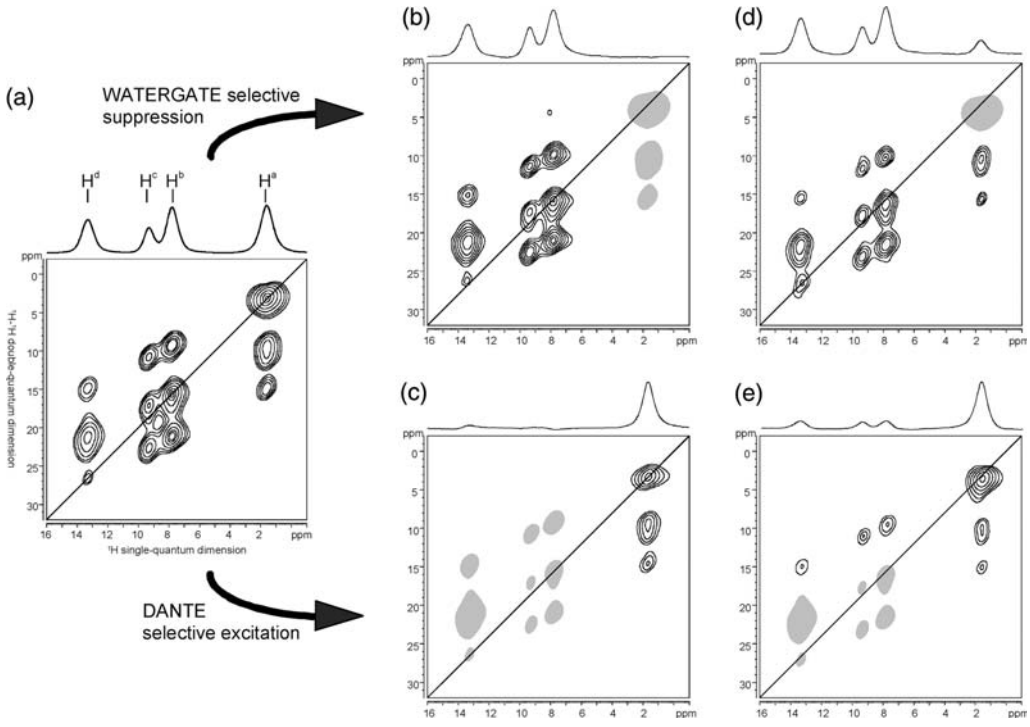

Fig. 7. Two-dimensional ^{1}H–^{1}H double-quantum NMR spectra of imidazolium-methylsulfonate, recorded under MAS by applying the pulse sequences depicted in Figs. 6a–e, respectively. The shaded spots indicate where DQ peaks are completely removed from the spectrum due to the selection procedure.

In Fig. 7a, the ^1H–^1H DQ spectrum of imidazoliummethylsulfonate is shown. Peaks corresponding to all possible DQ coherences are observed in the spectrum. This is expected for small molecules in a crystalline environment, because all types of protons are located in the vicinity of a given proton within an distance range of < 0.35nm. Only the signals of the H^d–H^d and H^c–H^c coherences are significantly weaker, because there is only one H^c and H^d proton per molecule, so that the coherences rely on intermolecular (and, thus, slightly more remote) ^1H–^1H contacts.

PFG-assisted WATERGATE and DANTE filters were incorporated into the DQ pulse sequence depicted in Fig. 6a. Two positions were chosen for inserting either a WATERGATE peak-suppression sequence or a DANTE selective peak–excitation sequence: (i) before detecting the signal in the t_2 dimension, and (ii) before exciting the DQ coherences. In case (i) only those DQ signals are detected/suppressed which are located on the resonance position of the selected proton species in the second (SQ) dimension, while in case (ii) only those DQ coherences are excited/suppressed in which the selected proton species is involved. In the latter case, full excitation/suppression is achieved when the DQ coherences involve only the selected protons species, whereas for mixed coherences partial excitation/suppression is observed (see below). The four variants of the pulse sequence are schematically displayed in Figs. 6b–d, while Figs. 7b–d show the experimental ^1H–^1H DQ spectra recorded with the respective pulse sequence. In Fig. 7b–d, the frequency selection was placed on the methyl (H^a) peak, but the experiments performed equally well on all four ^1H resonances. As the peak selection is efficiently achieved in a single transient of the PFG-assisted WATERGATE and DANTE sequences, the overall pulse sequence is applied with the same phase cycle as the non-selective DQ experiment (Fig. 6a). The filtering sequence is simply inserted into the pulse sequences, and the frequency-selective pulse is phase-cycled together with the pulses in which it is embedded.

The selective suppression and observation of a single ^1H resonance in the SQ dimension is readily accomplished by the WATERGATE and DANTE filter, respectively, and the spectra (Figs. 7b and c) are straightforward to understand: In Fig. 7b, all DQ peaks disappear from the spectrum at the suppressed SQ resonance frequency, while in Fig. 7c only those DQ signals are visible which are located at the selectively detected SQ resonance frequency. As the spectra in Fig. 7b and c are complementary to each other, their sum corresponds to the "full" DQ spectrum shown in Fig. 7a.

The selective excitation of DQ coherences by selecting or suppressing a peak immediately before the DQ excitation period works equally well, as can be inferred from Fig. 7d and e. For interpreting the spectra, it should be noted that a DQ coherence of a spin pair *A–B* can equally be generated starting from spin *A* and spin *B*. Consequently, when spin *A* is suppressed, *A–B* DQ coherences are still excited via spin *B*, but they lack about half the signal intensity. Analogously, when spin *A* is selectively excited, *A–B* type DQ coherences will also be observed, but again with only half the intensity as compared to the "fully excited" DQ spectrum. Only *A–A* type DQ coherences are completely removed from the spectrum (or present at full intensity), when spin *A* is suppressed before excitation (or selectively excited). With this in mind, the DQ spectra in Fig. 7d and e can be easily understood, and the experimental spectra indeed resemble all features that are expected when the filtering procedures are applied.

Thus, the two-dimensional ^1H–^1H DQ spectra nicely demonstrate that PFG-assisted WATERGATE and DANTE filters can straightforwardly and efficiently be used under fast MAS to remove unwanted signals or to selective excite signals of interest.

5. Examples: applications to supramolecular systems

In this section, two examples are given where the PFG-assisted WATERGATE filter is applied for suppressing a strong aliphatic ^1H signal. The materials under investigation are supramolecular systems which self-assemble into well-defined structures by means of non-covalent interactions, which are in our cases hydrogen bonds and π–π stacking. Solid-state ^1H NMR spectroscopy has proven to be very powerful and versatile for studying these types of interactions [50–53]. In the case of hydrogen bonds, the ^1H chemical-shift can be directly correlated with the strength of the bond [54]. For the investigation of π–π stacking phenomena, ^1H chemical shifts can serve as probes for π-electron densities nearby the respective proton, because the π-electrons have significant influence on the effective shielding experienced by the proton [55]. In this way, protons can be located relative to π-electron systems, and the arrangement of π–π stacks can be elucidated.

To be able to use ^1H chemical shifts for studies of hydrogen bonds and π–π stacks, ^1H resonance lines need to be spectrally resolved in the range of $\sim 5 \ldots 10$ ppm for π-electron shifts and $\sim 9 \ldots 15$ ppm for hydrogen bonds. Typically, the protons of interest for such studies constitute only a very minor fraction of the overall proton content of the material. In many organic systems, long alkyl sidechains are present, whose intense NMR signal strongly perturbs the observation of weaker resonances at higher frequencies in the spectra. When such alkyl chains are, in addition, significantly mobile, the situation is exacerbated in two-dimensional NMR spectra because motionally induced relaxation effects and coherence losses lead to intense noise (so-called t_1 noise) along the indirect dimension of the spectra. Such strong

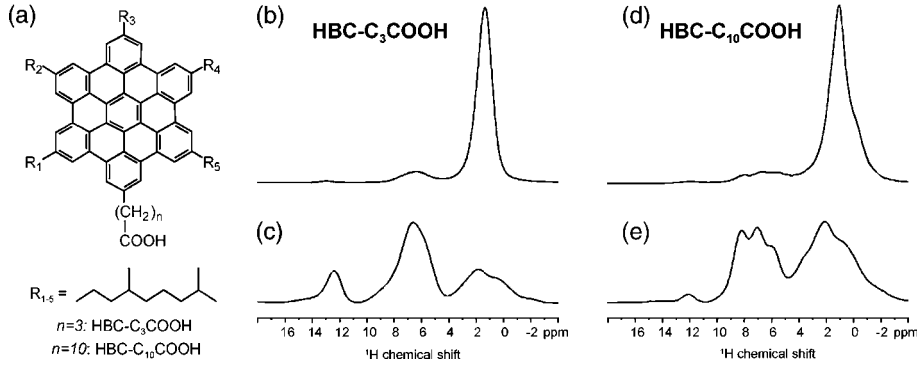

Fig. 8. (a) Two hexabenzocoronene derivatives with alkyl sidechains and a single carboxylic acid function at the end of one chain. The two materials only differ in the length of the chain carrying the carboxylic acid function. (b)–(e) ^{1}H MAS spectra of (a) recorded under MAS at 30 kHz. Regular spectra (b) and (d) are dominated by the intense alkyl ^{1}H signal, which can be suppressed by a PFG-assisted WATERGATE sequence (Fig. 2a) to yield spectra (c) and (e), in which the weaker aromatic and acidic ^{1}H signals of interest are much more pronounced.

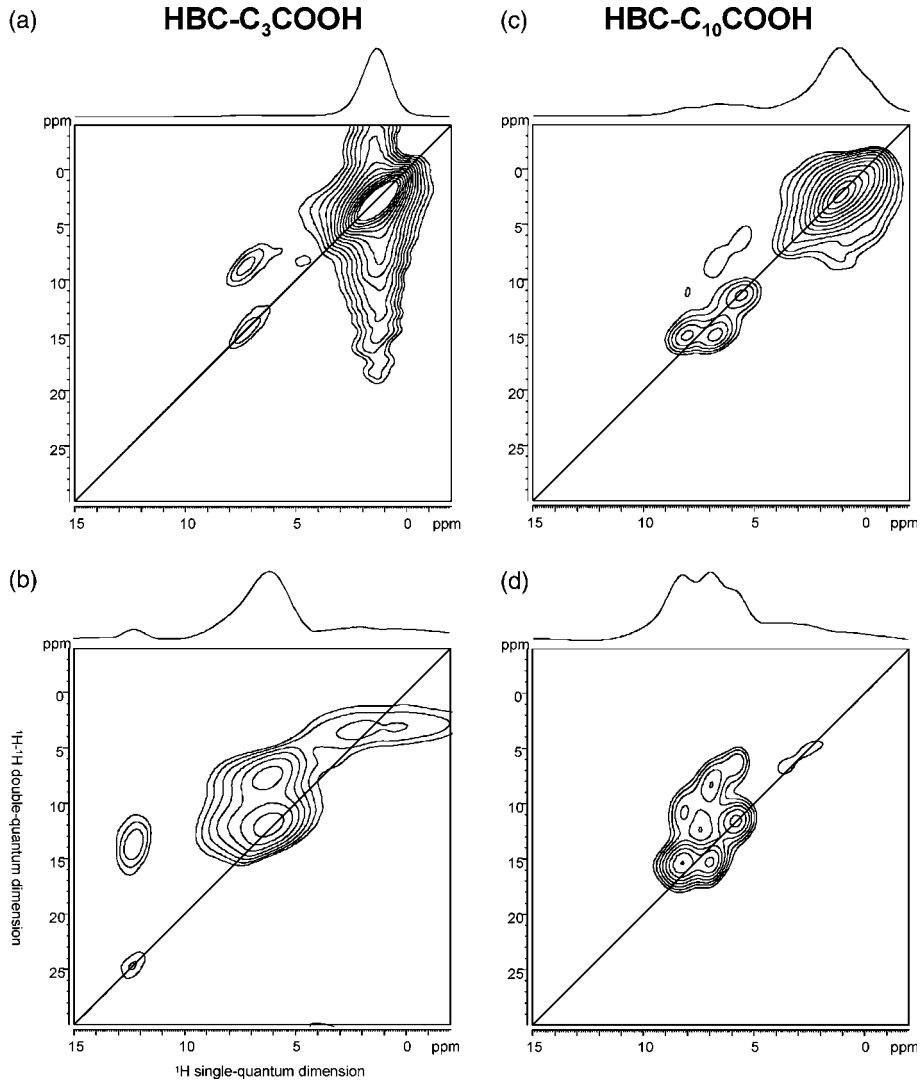

Fig. 9. ^{1}H–^{1}H double quantum spectra of the hexabenzocoronene acid derivatives depicted in Fig. 8a. The spectra are recorded under 30 kHz MAS, using the back-to-back sequence in Fig. 6a for (a) and (c) and the WATERGATE-assisted sequence in Fig. 6b for (b) and (d). With the strong alkyl signal being suppressed, the aromatic and acidic signals of interest are more conveniently accessible. The weak acidic ^{1}H–^{1}H double-quantum coherence in spectrum (b) is only observed when the strong alkyl signal is removed.

peaks, in particular in the combination with their noise, tend to obscure weaker resonances and to hamper the interpretation of the spectra. Problems of this kind can readily be solved by a peak-selective suppression technique, such as the PFG-assisted WATERGATE filter described above.

5.1. Hexabenzocoronene alkyl acid derivatives

As a first example, we consider ^{1}H NMR spectra of a two alkylated hexabenzocoronene (HBC) derivatives whose structure is depicted in Fig. 8a. The disc-shaped HBC cores are known to form solid discotic phases with two types of columnar stacks that differ in the angle between the disc-shaped molecule and the columnar axis [56,57]. The discs are either oriented perpendicular to the column (planar stack) or inclined at a tilt angle (herringbone-type stack). In addition, the carboxylic acid function enables the molecules to form hydrogen-bonded dimers [52]. The two materials investigated here differ only in the length of the *n*-alkyl chain that links the carboxylic acid function to the HBC core. Both hydrogen-bond formation and π–π stacking can be investigated by ^{1}H–^{1}H DQ NMR spectroscopy. When the discs stack in a herringbone fashion, a characteristic three-peak pattern is expected in the aromatic region of the DQ spectra [51,55] and when the molecules dimerise through hydrogen bonds, DQ signals will prove the existence of hydrogen-bonded pairs of acidic protons [52].

In Figs. 8b–e, ^{1}H MAS spectra of the two materials are shown, recorded at a spinning frequency of 30 kHz. In Figs. 8c and e, the intense signals of the $C_{11}H_{23}$ alkyl sidechains are reduced by the PFG-assisted WATERGATE technique (see Fig. 2a with $d_G = 33$ μs, $p_G = 100$ μs, $d'_G = 100$ μs, $d_W = 16.7$ μs, $\Delta B = 20$ G/cm) with an experimental efficiency of ~95–98%, meaning that only ~2–5% of the initial alkyl intensity is left. With the alkyl signals being suppressed, the receiver unit can be properly adjusted according to the signal intensities of the aromatic and acidic protons. DQ spectra were recorded without and with alkyl peak suppression using the pulse sequences depicted in Fig. 6a and b, respectively. As shown in Fig. 9, the DQ signals of interest can better be accessed and interpreted once the dominating alkyl peak is removed or, at least, largely reduced. In the case of HBC–C_3COOH, the DQ coherence of two acid protons (i.e. the peak located at 24/12 ppm), which serves as a clear evidence for the existence of hydrogen-bonded pairs of carboxylic acid groups, becomes only visible after alkyl signal suppression. Note that for HBC–C_{10}COOH, such a DQ coherence involving two acidic protons is not observed, which indicates that no stable hydrogen-bonded dimers are formed.

In the aromatic region, the DQ signals become much more prominent in the WATERGATE DQ spectra (see Figs. 9b and d), although it is, in principle, possible to identify and interpret them in the conventional DQ spectra (Fig. 9a and c). The characteristic pattern of three aromatic DQ peaks observed for HBC–C_{10}COOH shows that the HBC cores stack in a tilted herringbone-type fashion, while the broad and featureless aromatic DQ peak found for HBC–C_3COOH indicates a planar stacking. Obviously, the presence of strongly hydrogen-bonded dimers prevents the HBC cores in the columns from tilting. A complete study of these materials by solid-state NMR and X-ray scattering will be published elsewhere [58].

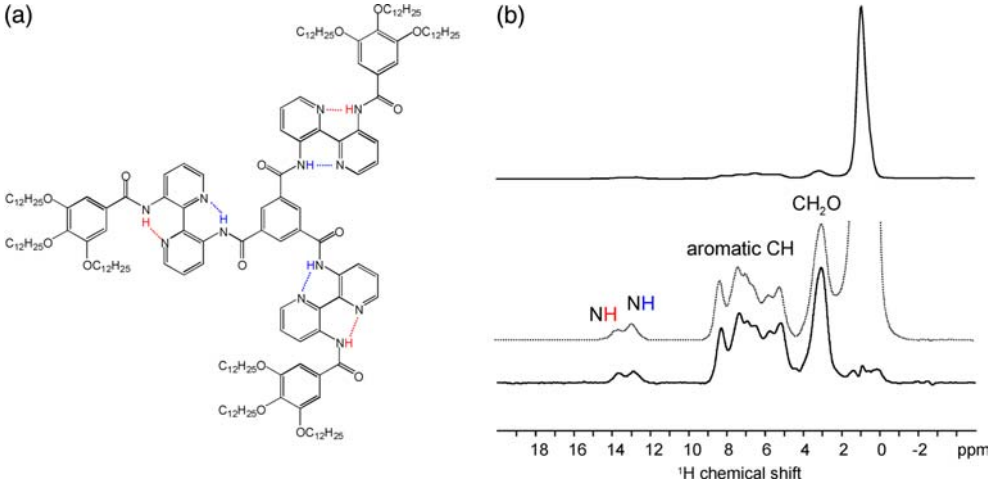

Fig. 10. (a) Chemical structure of a large discotic trisamide, which forms a liquid crystalline phase with hexagonally ordered columns at room temperature. (b) ^{1}H MAS spectra of (a). The single-pulse spectrum (top) is dominated by the intense signal of the long alkyl sidechains. Using a PFG-assisted WATERGATE sequence, the alkyl peak can be efficiently removed in a single transient (bottom spectrum), and the intensities of the other peaks remain unaffected, as can be seen from comparing the WATERGATE spectrum with a MAS spin–echo spectrum (dotted line), which accounts for slight transverse relaxation effects occurring during the echo delays.

5.2. Discotic trisamides

As a second example, we turn to another system that also associates into supramolecular stacks via π–π interactions [59]. It consists of C_3-symmetrical molecules with intramolecular hydrogen bonds (see Fig. 10a) and forms a discotic liquid–crystalline phase at room temperature with hexagonally ordered columns. At the periphery, nine n-$C_{12}H_{25}$ sidechains are attached which give rise to an intense alkyl peak in ^{1}H NMR spectra (see Fig. 10b, top spectrum). Moreover, in the liquid–crystalline phase the alkyl chains are very mobile, in particular towards their dangling ends, so that coherence losses due to motionally induced relaxation processes and, thus, strong t_1 noise in 2D NMR spectra are to be expected. To study aspects of molecular conformation and columnar stacking by NMR, however, the small signals of the aromatic CH- and amide NH-protons need to be accessed.

In Fig. 10b, two ^{1}H MAS spectra of the material are compared. Under MAS at 30 kHz, the ^{1}H resonance lines can nicely be resolved, but the conventional ^{1}H spectrum (top) is dominated by the intense alkyl peak that exceeds the other signals by more than a factor of 20. Applying a PFG-assisted WATERGATE sequence (depicted in Fig. 2a with $d_G = 33$ μs, $p_G = 100$ μs, $d'_G = 100$ μs, $d_W = 67$ μs, $\Delta B = 20$ G/cm), the alkyl peak can efficiently be suppressed, while all other signals are virtually unaffected, as can be seen from comparing the WATERGATE spectrum (bottom of Fig. 10b) to a normal MAS spin–echo spectrum (shown above as a dotted line). The PFG-WATERGATE spectrum was obtained from a *single* transient of the experiment and conveniently provides the ^{1}H signals of interest, including the NH resonances at 12.9 and 13.7 ppm. These high-frequency shifts clearly indicate the presence of strong N–H···N hydrogen bonds. As a side aspect, it should be noted that, when comparing the WATERGATE spectrum to a single-pulse spectrum, there are slight intensity distortions observed among the CH aromatic resonances due to transverse relaxation effects occurring during the echo delay.

Turning to ^{1}H–^{1}H DQ spectra (shown in Fig. 11), which aid the assignment of the various aromatic peaks, it becomes obvious that the strong t_1 noise arising from the intense signal of the mobile alkyl chains means a considerable disruption to the normal 2D spectrum (Fig. 11a), recorded using the back-to-back pulse sequence depicted in Fig. 6a. The t_1 noise is quite widely spread around the alkyl resonance and occurs at an intensity level which is comparable to that of the DQ signals of interest, so that a few of them are distorted or even completely obscured. By applying the pulse sequence depicted in Fig. 6b instead, the alkyl signal, together with its noise, can efficiently be removed from the spectrum (Fig. 11b) and the contacts between NH and

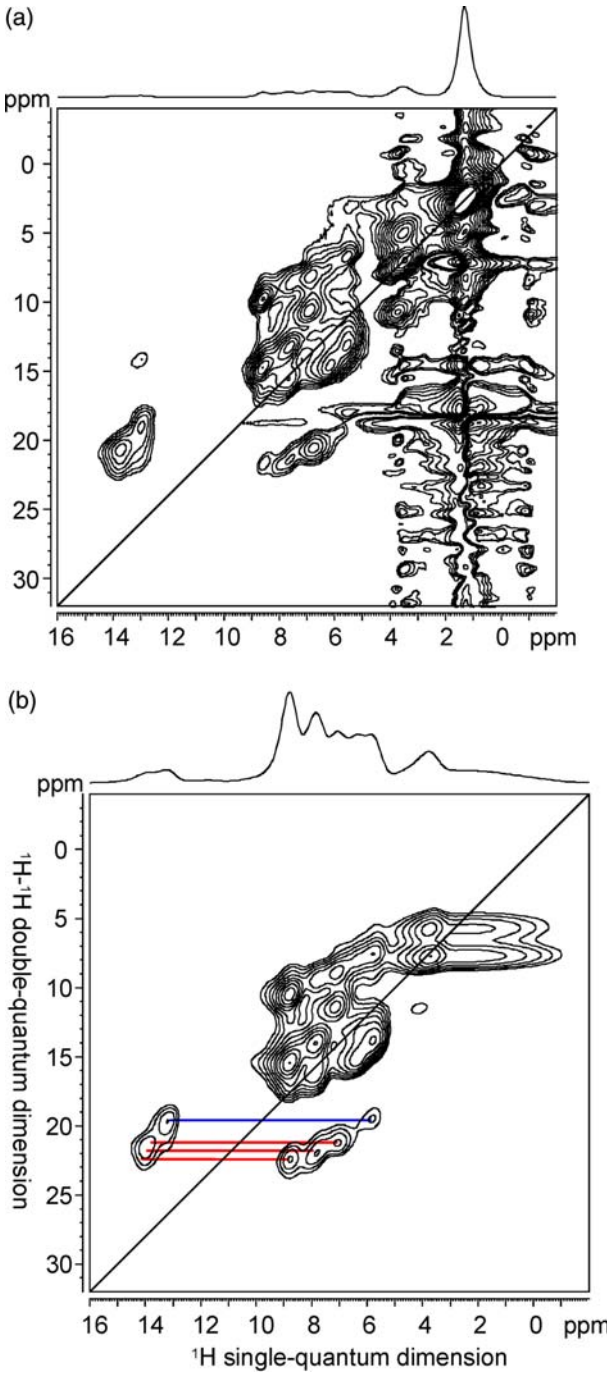

Fig. 11. ^{1}H–^{1}H double quantum spectra of the discotic trisamide depicted in Fig. 10a. The spectra are recorded under 30 kHz MAS, using the back-to-back sequence (shown in Fig. 6a) for (a) and the WATERGATE-assisted sequence (shown in Fig. 6b) for (b). In the regular DQ spectrum, the long alkyl chains give rise to intense t_1 noise due to motionally induced relaxation processes occurring during the pulse sequence. By use of WATERGATE peak suppression, the alkyl signal and its noise can be removed, so that the weak DQ signals of interest become conveniently accessible. The red and blue lines connect peaks that belong to DQ coherences between one of the two amide-NH protons and different aromatic–CH protons.

CH as well as among the CH protons can cleanly be identified and analysed.

Just to briefly explain the DQ coherences between NH and CH protons, it is found that the 13.7 ppm NH protons are involved in three such DQ coherences (marked red in Fig. 11b), while the 12.9 ppm NH protons form only one type of DQ coherence with the CH protons at 5.8 ppm. From this observation, the 12.9 ppm NH resonance can be assigned to the inner N–H···N hydrogen bonds in the structure (Fig. 10a), because at the inner NH location only the CH protons of the central phenyl ring are close enough in space to give rise to a NH–CH DQ coherence. At the outer NH location, in contrast, more CH protons are available in close proximity. A full analysis of the ^{1}H solid-state NMR spectra of this material is underway and will be presented elsewhere.

6. Conclusion and outlook

Techniques for frequency-selective excitation and suppression of ^{1}H NMR signals were adapted from liquid-/solution-state conditions to solid-state fast-MAS experiments. Frequency selection is accomplished by narrowband inversion pulses that are based on the well-established DANTE concept. Fast MAS is an essential requirement for such frequency-selection procedures to be applied in ^{1}H solid-state NMR, because they inherently rely on spectral resolution and, thus, on homonuclear dipolar decoupling. The efficiency of the selection or suppression can be drastically enhanced by PFGs, which in particular provide clean spectral selection in a single transient of the pulse sequence. In conventional fast-MAS probes, such gradients can be built by attaching a pair of coils to the top and the bottom of the MAS stator. From a practical point of view, coils of this design can easily be installed in MAS probes without significant modifications, but the coil geometry is not perfectly adapted to MAS conditions [34]. The selection efficiency achieveable with this simple coil design is in the order of 1%, which is perfectly sufficient for the homonuclear ^{1}H experiments demonstrated here. WATERGATE- or DANTE-type filter sequences can be readily incorporated into multidimensional ^{1}H NMR experiments, as we have demonstrated here for ^{1}H–^{1}H DQ spectroscopy on a crystalline model system and two supramolecular materials. In addition, Chevelkov et al. recently reported the use of PFGs in a fast-MAS probe for solvent suppression in biological materials [60]. Further improvements of gradient efficiency can be expected when a more elaborate coil design is used.

With the simple gradient design used in this work, heteronuclear ^{1}H–X dipolar filter techniques can not solely rely on PFGs for signal selection, but require assistance by a two-step pulse phase cycle. Nevertheless, fully PFG-based ^{1}H–X correlation techniques are approaching the performance required for experiments on ^{13}C or ^{15}N in natural abundance. There is potential to develop such PFG techniques under fast MAS further towards ^{1}H-detected two-dimensional ^{1}H–X HSQC experiments that would significantly benefit from enhanced signal sensitivity, as could already be shown for ^{1}H-detected ^{1}H–^{15}N correlation experiments [46,60]. Thus, more methodological progress can be expected from the gradual convergence of solution- and solid-state NMR spectroscopy.

Acknowledgments

The authors thank N. Tchebotareva, M.D. Watson and K. Müllen (Mainz) as well as E.W. Meijer (Eindhoven) for providing the hexabenzocoronene and trisamide samples, respectively. Financial support by the Deutsche Forschungsgemeinschaft (SFB 625) is gratefully acknowledged, and K.T. thanks the Fond der Chemischen Industrie for a graduate fellowship.

References

[1] R. Freeman, Selective excitation in high-resolution NMR, Chem. Rev. 91 (1991) 1397–1412.
[2] R. Freeman, High resolution NMR using selective excitation, J. Mol. Struct. 266 (1992) 39–51.
[3] E. Kupce, R. Freeman, Techniques for multisite excitation, J. Magn. Reson. A 105 (1993) 234–238.
[4] E. Kupce, R. Freeman, Polychromatic selective pulses, J. Magn. Reson. A 102 (1993) 122–126.
[5] P.J. Hore, Solvent suppression in Fourier transform nuclear magnetic resonance, J. Magn. Reson. 55 (1983) 283–300.
[6] M. Gueron, P. Plateau, M. Decorps, Solvent signal suppression in NMR, Progr. Nucl. Magn. Reson. Spectr. 23 (1991) 135–209.
[7] C. Bauer, R. Freeman, T. Frenkiel, J. Keeler, A.J. Shaka, Gaussian pulses, J. Magn. Reson. 58 (1984) 442–457.
[8] H. Geen, R. Freeman, Band-selective radiofrequency pulses, J. Magn. Reson. 93 (1991) 93–141.
[9] S. Berger, NMR techniques employing selective radiofrequency pulses in combination with pulsed field gradients, Progr. Nucl. Magn. Reson. Spectr. 30 (1997) 137–156.
[10] M. Sattler, J. Schleucher, C. Griesinger, Heteronuclear multidimensional NMR experiments for the structure determination of proteins in solution employing pulsed field gradients, Progr. NMR Spectr. 34 (1999) 93–158.
[11] M.A. Bernstein, L.A. Trimble, High-resolution NMR experiments which use frequency-selective RF pulses in combination with magnetic-field gradients, Magn. Reson. Chem. 32 (1994) 107–110.
[12] V. Sklenar, Z. Starcuk, 1–2–1 pulse train: a new effective method of selective excitation for proton NMR in water, J. Magn. Reson. 50 (1982) 495–501.
[13] G.M. Clore, B.J. Kimber, A.M. Gronenborn, The 1–1 hard pulse: a simple and effective method of water resonance suppression in FT ^{1}H NMR, J. Magn. Reson. 54 (1983) 170–173.
[14] G. Bodenhausen, R. Freeman, G.A. Morris, Simple pulse sequence for selective excitation in Fourier-transform NMR, J. Magn. Reson. 23 (1976) 171–175.

[15] R. Freeman, A Handbook of Nuclear Magnetic Resonance, Longman, Harlow, 1987, pp. 207–215.
[16] M. Piotto, V. Saudek, V. Sklenar, Gradient-tailored excitation for single-quantum NMR spectroscopy of aqueous solutions, J. Biomol. NMR 2 (1992) 661–665.
[17] V. Sklenar, M. Piotto, R. Leppik, V. Saudek, Gradient-tailored water suppression for ^{1}H–^{15}N HSQC experiments optimized to retain full sensitivity, J. Magn. Reson. Ser. A 102 (1993) 241–245.
[18] D. Turner, Binomial solvent suppression, J. Magn. Reson. 54 (1983) 146–148.
[19] E. Kupce, R. Freeman, Binomial filters, J. Magn. Reson. 99 (1992) 644–651.
[20] C. Wang, A. Pardi, NMR spectra of exchangeable protons using uniform excitation solvent suppression pulse sequences, J. Magn. Reson. 71 (1987) 154–158.
[21] R. Freeman, Shaped radiofrequency pulses in high resolution NMR, Progr. Nucl. Magn. Reson. Spectr. 32 (1998) 59–106.
[22] L. Emsley, Selective pulses and their applications to assignment and structure determination in nuclear magnetic resonance, Method Enzymol. 239 (1994) 207–246.
[23] K.E. Cano, M.A. Smith, A.J. Shaka, Adjustable, broadband, selective excitation with uniform phase, J. Magn. Reson. 155 (2002) 131–139.
[24] D.G. Cory, J.W.M.v. Os, W.S. Veeman, MAS imaging, J. Magn. Reson. 76 (1989) 543.
[25] C.A. Fyfe, J. Skibsted, H. Grondey, H. Meyer, Pulsed field gradient multiple quantum MAS NMR spectroscopy of half-integer spin quadrupolar nuclei, Chem. Phys. Lett. 281 (1998) 44.
[26] W.E. Maas, A. Bielecki, M. Ziliox, F.H. Laukien, D.G. Cory, Magnetic field gradients in solid state magic angle spinning NMR, J. Magn. Reson. 141 (1999) 29–33.
[27] T. Fritzhanns, S. Hafner, D.E. Demco, H.W. Spiess, F.H. Laukien, Pulsed field gradient selection in two-dimensional magic angle spinning NMR spectroscopy of dipolar solids, J. Magn. Reson. 134 (1998) 355–359.
[28] P.A. Keifer, High-resolution NMR techniques for solid-phase synthesis and combinatorial chemistry, Drug Discovery Today 2 (1997) 468–478.
[29] M.J. Shapiro, J.R. Wareing, NMR methods in combinatorial chemistry, Curr. Opin. Chem. Biol. 2 (1998) 372–375.
[30] G. Lippens, M. Bourdonneau, C. Dhalluin, R. Warrass, T. Richert, C. Seetharaman, C. Boutillon, M. Piotto, Study of compounds attached to solid supports using high resolution magic angle spinning NMR, Curr. Org. Chem. 3 (1999) 147.
[31] C. Dhalluin, C. Boutillon, A. Tartar, G. Lippens, Magic angle spinning nuclear magnetic resonance in solid-phase peptide synthesis, J. Am. Chem. Soc. 119 (1997) 10494.
[32] R. Warrass, J.M. Wieruszeski, C. Boutillon, G. Lippens, High-resolution magic angle spinning NMR study of resin-bound polyalanine peptides, J. Am. Chem. Soc. 122 (2000) 1789.
[33] J. Furrer, M. Piotto, M. Bourdonneau, D. Limal, G. Guichard, K. Elbayed, J. Raya, J.P. Briand, A.J. Bianco, Evidence of secondary structure by high-resolution magic angle spinning NMR spectroscopy of a bioactive peptide bound to different solid supports, J. Am. Chem. Soc. 123 (2001) 4130.
[34] W.E. Maas, F.H. Laukien, D.G. Cory, Gradient, high-resolution, magic-angle sample spinning NMR, J. Am. Chem. Soc. 118 (1996) 13085–13086.
[35] T. Gullion, J. Schaefer, Rotational-echo double-resonance NMR, J. Magn. Reson. 81 (1989) 196–200.
[36] T. Gullion, J. Schaefer, Detection of weak heteronuclear dipolar coupling by rotational-echo double-resonance nuclear magnetic resonance, Adv. Magn. Reson. 13 (1989) 57–83.
[37] T. Gullion, Introduction to rotational-echo, double-resonance NMR, Concepts Magn. Reson. 10 (1998) 277–289.
[38] D. Boudot, D. Canet, J. Brondeau, J.C. Boubel, DANTE-Z—a new approach for accurate frequency-selectivity using hard pulses, J. Magn. Reson. 83 (1989) 428–439.
[39] A.W. Hing, S. Vega, J. Schaefer, Transferred-echo double-resonance NMR, J. Magn. Reson. 96 (1992) 205–209.
[40] K. Saalwächter, R. Graf, H.W. Spiess, Recoupled polarization transfer heteronuclear ^{1}H–^{13}C multiple-quantum correlation in solids under ultra-fast MAS, J. Magn. Reson. 140 (1999) 471–476.
[41] K. Saalwächter, R. Graf, H.W. Spiess, Recoupled polarization-transfer methods for solid-state ^{1}H–^{13}C heteronuclear correlation in the limit of fast MAS, J. Magn. Reson. 148 (2001) 398–418.
[42] K. Saalwächter, H.W. Spiess, Heteronuclear ^{1}H–^{13}C multiple-spin correlation in solid-state NMR: combining REDOR recoupling and multiple-quantum spectroscopy, J. Chem. Phys. 114 (2001) 5707–5728.
[43] Y. Ishii, R. Tycko, Sensitivity enhancement in solid state N-15 NMR by indirect detection with high-speed magic angle spinning, J. Magn. Reson. 142 (2000) 199–204.
[44] Y. Ishii, J.P. Yesinowski, R. Tycko, Sensitivity enhancement in solid-state C-13 NMR of synthetic polymers and biopolymers by H-1 NMR detection with high-speed magic angle spinning, J. Am. Chem. Soc. 123 (2001) 2921–2922.
[45] I. Schnell, B. Langer, S.H.M. Söntjens, M.H.P. van Genderen, R.P. Sijbesma, H.W. Spiess, Inverse detection and heteronuclear editing in ^{1}H–^{15}N correlation and ^{1}H–^{1}H double-quantum NMR spectroscopy in the solid state under fast MAS, J. Magn. Reson. 150 (2001) 57–70.
[46] I. Schnell, K. Saalwächter, ^{15}N–^{1}H bond length determination in natural abundance by inverse detection in fast-MAS solid-state NMR spectroscopy, J. Am. Chem. Soc. 124 (2002) 10938–10939.
[47] K. Saalwächter, I. Schnell, REDOR-based heteronuclear dipolar correlation experiments in multi-spin systems: rotor-encoding, directing, and multiple distance and angle determination, Solid State Nucl. Magn. Reson. 22 (2002) 154–187.
[48] I. Schnell, H.W. Spiess, High resolution ^{1}H NMR spectroscopy in the solid state: very fast sample rotation and multiple-quantum coherences, J. Magn. Reson. 151 (2001) 153–227.
[49] M. Feike, D.E. Demco, R. Graf, J. Gottwald, S. Hafner, H.W. Spiess, Broadband multiple-quantum NMR spectroscopy, J. Magn. Reson. A 122 (1996) 214–221.
[50] I. Schnell, S.P. Brown, H.Y. Low, H. Ishida, H.W. Spiess, An investigation of hydrogen bonding in benzoxazine dimers by fast magic-angle spinning and double-quantum ^{1}H NMR spectroscopy, J. Am. Chem. Soc. 120 (1998) 11784–11795.
[51] S.P. Brown, I. Schnell, J.D. Brand, K. Müllen, H.W. Spiess, An investigation of π–π packing in a columnar hexabenzocoronene by fast magic-angle spinning and double-quantum ^{1}H solid-state NMR spectroscopy, J. Am. Chem. Soc. 121 (1999) 6712–6718.
[52] S.P. Brown, I. Schnell, J.D. Brand, K. Müllen, H.W. Spiess, The competing effects of π–π packing and hydrogen bonding in a hexabenzocoronene carboxylic acid derivative: a ^{1}H solid-state MAS NMR investigation, Phys. Chem. Chem. Phys. 2 (2000) 1735–1745.
[53] S.P. Brown, H.W. Spiess, Advanced solid-state NMR methods for the elucidation of structure and dynamics of molecular, macromolecular, and supramolecular systems, Chem. Rev. 101 (2001) 4125–4155.
[54] R.K. Harris, in: D.M. Grant, R.K. Harris (Eds.), Encyclopedia of Nuclear Magnetic Resonance, vol. 5, Wiley, Chichester, 1996, p. 3314.
[55] C. Ochsenfeld, S.P. Brown, I. Schnell, J. Gauss, H.W. Spiess, Structure assignment in the solid state by the coupling of quantum chemical calculations with NMR experiments: a columnar hexabenzocoronene derivative, J. Am. Chem. Soc. 123 (2001) 2597–2606.

[56] M.D. Watson, A. Fechtenkötter, K. Müllen, Big is beautiful—'aromaticity' revisited from the viewpoint of macromolecular and supramolecular benzene chemistry, Chem. Rev. 101 1267–1300.
[57] I. Fischbach, T. Pakula, P. Minkin, A. Fechtenkötter, K. Müllen, H.W. Spiess, K. Saalwächter, Structure and dynamics in columnar discotic materials: a combined X-ray and solid-state NMR study of hexabenzocoronene derivatives, J. Phys. Chem. B 106 (2002) 6408–6418.
[58] N. Tchebotareva, I. Fischbach, M.D. Watson, I. Schnell, K. Müllen, H.W. Spiess, in preparation.
[59] J.J. van Gorp, J.A.J.M. Vekemans, E.W. Meijer, C-3-symmetrical supramolecular architectures: fibers and organic gels from discotic trisamides and trisureas, J. Am. Chem. Soc. 124 (2002) 14759–14769.
[60] V. Chevelkov, B.J. van Rossum, F. Castellani, K. Rehbein, A. Diehl, M. Hohwy, S. Steuernagel, F. Engelke, H. Oschkinat, B. Reif, ^{1}H detection in MAS solid-state NMR spectroscopy of biomacromolecules employing pulsed field gradients for residual solvent suppression, J. Am. Chem. Soc. 125 (2003) 7788–7789.